

A novel car-following model by sharing cooperative information transmission delayed effect under V2X environment and its additional energy consumption

Guang-Han Peng(彭光含), Te-Ti Jia(贾特提), Hua Kuang(邝华), Hui-Li Tan(谭惠丽), and Tao Chen(陈陶)
Citation: Chin. Phys. B, 2022, 31 (**5**): 058901. DOI: 10.1088/1674-1056/ac422a
Journal homepage: http://cpb.iphy.ac.cn; http://iopscience.iop.org/cpb

What follows is a list of articles you may be interested in

CO_2 emission control in new CM car-following model with feedback control of the optimal estimation of velocity difference under V2X environment

Guang-Han Peng(彭光含), Rui Tang(汤瑞), Hua Kuang(邝华), Hui-Li Tan(谭惠丽), and Tao Chen(陈陶)
Chin. Phys. B, 2021, 30 (**10**): 108901. DOI: 10.1088/1674-1056/ac1417

Influence of bottleneck on single-file pedestrian flow: Findings from two experiments

Cheng-Jie Jin(金诚杰), Rui Jiang(姜锐), Da-Wei Li(李大韦)
Chin. Phys. B, 2020, 29 (**8**): 088902. DOI: 10.1088/1674-1056/ab8da3

A new cellular automaton model accounting for stochasticity in traffic flow induced by heterogeneity in driving behavior

Xiaoyong Ni(倪晓勇), Hong Huang(黄弘)
Chin. Phys. B, 2019, 28 (**9**): 098901. DOI: 10.1088/1674-1056/ab343b

Effects of rainy weather on traffic accidents of a freeway using cellular automata model

Ming-Bao Pang(庞明宝), Bo-Ning Ren(任泊宁)
Chin. Phys. B, 2017, 26 (**10**): 108901. DOI: 10.1088/1674-1056/26/10/108901

Influence of bus stop with left-turn lines between two adjacent signalized intersections

Ming-Bao Pang(庞明宝), Lan-Hang Ye(叶兰杭), Ya-Nan Pei(裴亚男)
Chin. Phys. B, 2016, 25 (**8**): 088901. DOI: 10.1088/1674-1056/25/8/088901

A novel car-following model by sharing cooperative information transmission delayed effect under V2X environment and its additional energy consumption

Guang-Han Peng(彭光含)[1,†], Te-Ti Jia(贾特提)[1], Hua Kuang(邝华)[1], Hui-Li Tan(谭惠丽)[1], and Tao Chen(陈陶)[2]

[1] *College of Physical Science and Technology, Guangxi Normal University, Guilin* 541004, *China*
[2] *Boyuan Scientific Instruments (Zhenjiang) Co., Ltd, Zhenjiang* 212003, *China*

(Received 10 November 2021; revised manuscript received 10 November 2021; accepted manuscript online 11 December 2021)

A novel car-following model is offered based on the cooperative information transmission delayed effect involving headway and velocity under V2X environment. The stability conditions and mKdV equation of the new model are obtained via the linear and nonlinear analysis. Through numerical simulation, the variation trend of headway and hysteresis phenomenon are studied. In addition, we investigate the additional energy consumption of the vehicle during acceleration. In brief, theoretical analysis and simulation results confirm that the new car-following model based on the cooperative information transmission delayed effect can improve traffic stability and reduce additional energy consumption.

Keywords: traffic flow, car-following model, additional energy consumption

PACS: 89.40.–a, 05.70.Fh **DOI:** 10.1088/1674-1056/ac422a

1. Introduction

With the improvement of people's living standards, the speed of road construction is far lower than the growth rate of vehicles, which leads to increasingly worse traffic conditions, traffic congestion, and traffic safety problems. As the above traffic situation is becoming more and more serious, scholars have advanced many traffic models to analyze traffic behaviors and solve traffic congestion from different perspectives. Then, there have occurred the car-following models,[1–9] cellular automata models,[10–15] and lattice hydrodynamic models.[16–22] Among them, the optimal velocity (OV) model[3] is a classic car-following model. However, the OV model has some defects such as exorbitant acceleration and deceleration. Thereafter, Helbing and Tilch[23] brought forward a generalized force (GF) model. They used the vehicle tracking data to calibrate the OV model, solving the problems in the OV model. But the GF model cannot describe the delayed time and start-up velocity in real traffic. Afterwards, Jiang *et al.*[24] established a full velocity difference (FVD) model in regard of the difference between positive velocity and negative velocity, which made up for the defects of GF model. The research on the car-following model is still in-depth with the efforts of many scholars, who have made great contributions to the development of traffic flow.

More importantly, with the popularization of vehicle to X (V2X) communications technology, drivers can acquire traffic information such as the position and speed of surrounding themselves, as well as the average headway of vehicles from a macro perspective. Therefore, under V2X environment, real-time traffic data can be used to guide drivers to adjust their driving behavior. Backfrieder *et al.*[25] used V2X communication to detect, predict and solve traffic congestion problems. Zhang *et al.*[26] provided a comprehensive framework based on the V2X technology and built an unusual model to detect the driving behaviors on different roads. Ma *et al.*[27] proposed a traffic control system for ring roads under the V2X environment. Peng *et al.*[28] raised a CM car-following model by integrating the estimated optimal speed effect under the V2X environment. With the spread of 5G, the V2X technology could play a greater role in conveying the delayed information including headway and velocity.

Therefore, a novel car-following model in this paper is established by sharing cooperative information transmission delayed (CITD) effect covering headway and velocity of the current vehicle under the V2X environment. The rest of this paper is organized as follows. In Section 2, we will list some existing models about the delay feedback control in the field of traffic flow and explain the construction logic of the new model. The linear stability analysis and nonlinear stability analysis will be studied in Sections 3 and 4. The content of Section 5 is the numerical simulation, which includes the headway distribution and the hysteresis loop. In particular, the additional energy consumption is further studied with the consideration of the CITD effect. Finally, in Section 6, the corresponding conclusions are drawn.

[†]Corresponding author. E-mail: pengguanghan@163.com

© 2022 Chinese Physical Society and IOP Publishing Ltd

2. Extended car-following model

The OV model is a classic car-following model put forward by Bando *et al.*,[3] and its motion equation is shown below:

$$\frac{\mathrm{d}v_n(t)}{\mathrm{d}t} = a\left[V\left(\Delta x_n(t)\right) - v_n(t)\right], \tag{1}$$

where a signifies the sensitivity of the driver. The acceleration $\mathrm{d}v_n(t)/\mathrm{d}t$ of the n-th vehicle at time t is determined by the difference between the optimal velocity $\Delta V\left(x_n(t)\right)$ and the actual velocity $v_n(t)$. One adopts the optimal velocity as the following tangent function:[3]

$$V(\Delta x) = \frac{v_{\max}}{2}\left[\tanh(\Delta x - h_{\mathrm{c}}) + \tanh(h_{\mathrm{c}})\right], \tag{2}$$

where h_{c} represents the safe distance and $v_{\max}$ means the maximum velocity.

In recent years, the research and application of time-delay feedback control technology in the field of traffic flow have attracted the attention of some scholars.[29–43] In 2011, Ge[29] advanced a modified CM car-following model and its delayed feedback control scheme. In 2013, Jin and Hu[30] introduced a delayed feedback control of displacement and velocity difference based on the OV model. Wang *et al.*[33] presented a lattice model for the current lattice flow difference delay feedback control. Peng *et al.*[34] built a lattice model via considering the effect of historical density differences. Kaur and Sharma[36] put forward a feedback control model with transitive delay. Zhang *et al.*[39] raised an extended car-following model in which the continuous self-delay velocity of multiple preceding vehicles was taken into account. Jin and Meng[40] put forward an extended OV model with time-delay feedback control. Li *et al.*[41] studied an improved car-following model in view of electronic throttle dynamics and the delay of velocity difference. Guan *et al.*[42] offered a bifurcation control method based on the expected effect and response delay feedback. Recently, Li *et al.*[43] developed a car-following model by considering the influence of the historical velocity on traffic. Scholars realize that the time-delayed feedback control has great significance and engineering application value in transportation system.

Generally, the driving state of the vehicle in the car-following model is often determined by two important factors, namely, vehicle's headway and velocity, which have a significant influence on subsequent traffic evolution. But the previous models did not consider the CITD effect involving the headway and velocity. Therefore, a patulous car-following model is taken by sharing the CITD effect as

$$\begin{aligned}\frac{\mathrm{d}v_n(t)}{\mathrm{d}t} &= a\left\{V\left[\Delta x_n(t) + \kappa\left(\Delta x_n(t) - \Delta x_n(t-\tau)\right)\right] - v_n(t)\right\} \\ &\quad + a\lambda\left[v_n(t) - v_n(t-\tau)\right],\end{aligned} \tag{3}$$

where $\kappa\left(\Delta x_n(t) - \Delta x_n(t-\tau)\right)$ and $\lambda\left[v_n(t) - v_n(t-\tau)\right]$ express the delayed effect of headway and velocity, respectively; κ and λ are the control parameters correspondingly; τ is the delayed time which is equal to the inverse of a. And the new model recovers to the OV model if κ and λ are 0. Then, we compare new model with the OV model through theoretical analysis and numerical simulation.

3. Stability analysis

In order to facilitate the subsequent linear analysis, the new model is treated linearly. Using Taylor expansion, we can write the optimal velocity term in Eq. (3) as follows:

$$\begin{aligned}&V\left[\Delta x_n(t) + \kappa(\Delta x_n(t) - \Delta x_n(t-\tau))\right] \\ &= V(\Delta x_n(t)) + \kappa(\Delta x_n(t) - \Delta x_n(t-\tau))V'(\Delta x_n(t)).\end{aligned} \tag{4}$$

Equation (3) can be rewritten as

$$\begin{aligned}\frac{\mathrm{d}v_n(t)}{\mathrm{d}t} &= a\{V(\Delta x_n(t)) + \kappa(\Delta x_n(t) - \Delta x_n(t-\tau)) \\ &\quad \times V'(\Delta x_n(t)) - v_n(t)]\} + a\lambda[v_n(t) - v_n(t-\tau)].\end{aligned} \tag{5}$$

If the traffic on the road is stable, then all vehicles on the road will keep the same distance (that is, the headway h) and drive forward at the optimal velocity $V(h)$. The state can be expressed as

$$x_n^0(t) = hn + V(h)t, \quad h = L/N, \tag{6}$$

where N is the total number of vehicles on the road, L is the road length. Assume that $y_n(t)$ is a small disturbance of the steady state solution $x_n^0(t)$ then the following equation can be obtained:

$$x_n(t) = x_n^0(t) + y_n(t). \tag{7}$$

Subsequently,

$$\begin{aligned}\frac{\mathrm{d}^2 y_n(t)}{\mathrm{d}t^2} &= a[V'(h)\Delta y_n(t) + \kappa(\Delta y_n(t) - \Delta y_n(t-\tau))V'(h) \\ &\quad - \frac{\mathrm{d}y_n(t)}{\mathrm{d}t}] + a\lambda\left[\frac{\mathrm{d}y_n(t)}{\mathrm{d}t} - \frac{\mathrm{d}y_n(t-\tau)}{\mathrm{d}t}\right],\end{aligned} \tag{8}$$

where

$$\Delta y_n(t) = y_{n+1}(t) - y_n(t), \quad V'(h) = \left.\frac{\mathrm{d}V(\Delta x)}{\mathrm{d}\Delta x}\right|\Delta x = h.$$

By expanding $y_n = A\exp(\mathrm{i}kn + zt)$, we can obtain the following equation:

$$\begin{aligned}&z^2 + az - aV'(h)(\mathrm{e}^{\mathrm{i}k} - 1)[1 + \kappa(1 - \mathrm{e}^{z\tau})] \\ &+ a\lambda z(\mathrm{e}^{-z\tau} - 1) = 0.\end{aligned} \tag{9}$$

Expanding $z = z_1(\mathrm{i}k) + z_2(\mathrm{i}k)^2 + \cdots$, and ignoring terms with order higher than 2, we obtain

$$z_1 = V'(h), \tag{10}$$

$$z_2 = \frac{aV'(h) - 2z_1^2 + 2z_1^2\lambda + 2z_1\kappa V'(h)}{2a}. \tag{11}$$

At this point, the traffic flow is still steady when $z_2 > 0$. And the traffic flow tends to be unstable if $z_2 < 0$. Therefore, we gain the neutral stability condition of the new model below:

$$a = 2V'(h)(1-\kappa-\lambda). \tag{12}$$

The traffic flow is stable under small disturbances if the following inequality holds:

$$a > 2V'(h)(1-\kappa-\lambda). \tag{13}$$

It is obvious that the stable condition is consistent with the OV model[3] when $\kappa = 0$ and $\lambda = 0$. Figure 1 displays the neutral stability line of the relationship between headway and driver sensitivity under different values of control coefficient κ and λ (see the solid line). The peak value of each curve represents the critical point (h_c, a_c) in Fig. 1.

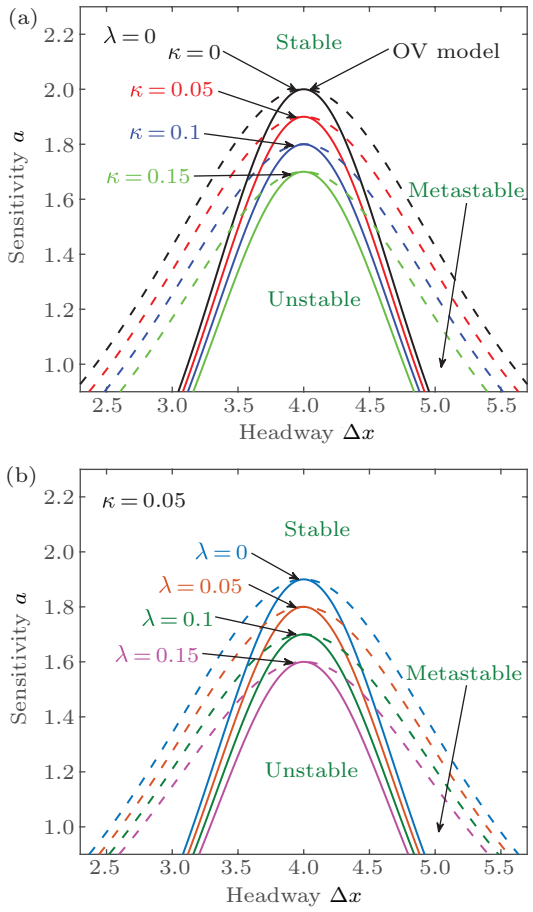


Fig. 1. Neutral stability curve and coexistence curve for (a) $\lambda = 0$ and various values of κ, and (b) $\kappa = 0.05$ and various values of λ.

The areas above the neutral curve are stable areas without traffic jams, while the areas below the neutral curve are unstable areas. Figure 1(a) describes the situation as κ increases when $\lambda = 0$. Evidently, the critical sensitivity a_c of the new model declines with the increase of κ, which implies that the stable area expands by considering the headway delayed effect. Furthermore, figure 1(b) displays the cases under different values of λ under the same control coefficient κ. Apparently, the neutral stability lines show a downward trend when λ goes up, which means that the stable area is also broadening and the traffic flow also changes in the direction of stability by strengthening the velocity delayed effect. Therefore, the results from linear analysis show that the stability of the transportation system can be significantly enhanced under the CITD effect covering the headway and velocity.

4. Nonlinear analysis

In order to study the influence of CITD effect on the evolution process of traffic flow density wave, we conduct the nonlinear analysis and obtain the mKdV equation describing the kink–antikink density wave. Above all, for the convenience of research, equation (5) is rewritten as

$$\begin{aligned}\frac{\mathrm{d}^2\Delta x_n(t)}{\mathrm{d}t^2} &= a\left[V(\Delta x_{n+1}(t)) - V(\Delta x_n(t)) - \frac{\mathrm{d}\Delta x_n(t)}{\mathrm{d}t}\right] \\ &\quad + aV'(h_c)\kappa[\Delta x_{n+1}(t) - \Delta x_n(t) \\ &\quad - (\Delta x_{n+1}(t-\tau) - \Delta x_n(t-\tau))] \\ &\quad + a\lambda\left[\frac{\mathrm{d}\Delta x_n(t)}{\mathrm{d}t} - \frac{\mathrm{d}\Delta x_n(t-\tau)}{\mathrm{d}t}\right].\end{aligned} \tag{14}$$

We introduce infinitesimal quantities ε and define slow scales X and T[44,45] at the same time as follows:

$$X = \varepsilon(n + bt), \quad T = \varepsilon^3 t, \quad \varepsilon\ (0 < \varepsilon \ll 1), \tag{15}$$

where b is a constant to be determined. The headway $\Delta x_n(t)$ is expressed as

$$\Delta x_n(t) = h_c + \varepsilon R(X, T). \tag{16}$$

Therefore, equation (14) can be expanded to the fifth order of ε as follows:

$$\begin{aligned}&\varepsilon^2(b - V')\partial_X R + \varepsilon^3\left[\frac{b^2}{a}(1-\lambda) - \left(\kappa b\tau + \frac{1}{2}\right)V'\right]\partial_X^2 R + \varepsilon^4\left\{\partial_T R + \frac{1}{6}[3\lambda b^3\tau^2 + (3\kappa b^2\tau^2 - 3\kappa b\tau - 1)V']\partial_X^3 R - \frac{1}{6}V'''\partial_X R^3\right\} \\ &+\varepsilon^5\left\{\left(\frac{2b}{a} - 2\lambda b\tau - \kappa\tau V'\right)\partial_X\partial_T R - \frac{1}{12}V'''\partial_X^2 R^3 - \frac{1}{24}[4\lambda b^4\tau^3 + (4\kappa b^3\tau^3 - 6\kappa b^2\tau^2 + 4\kappa b\tau + 1)V']\partial_X^4 R\right\} = 0.\end{aligned} \tag{17}$$

Here,

$$V' = \left.\frac{\mathrm{d}V(\Delta x_n)}{\mathrm{d}\Delta x_n}\right|\Delta x_n = h_c, \quad V''' = \left.\frac{\mathrm{d}^3V(\Delta x_n)}{\mathrm{d}\Delta x_n{}^3}\right|\Delta x_n = h_c.$$

Near the critical point (h_c, a_c), $a_c = a(1+\varepsilon^2)$. By taking $b = V'(h_c)$, ε^2 and ε^3can be eliminated in Eq. (17), *i.e.*,

$$\begin{aligned}&\varepsilon^4(\partial_T R - g_1\partial_X^3 R + g_2\partial_X R^3)\\&+\varepsilon^5(g_3\partial_X^2 R + g_4\partial_X^4 R + g_5\partial_X^2 R^3) = 0.\end{aligned} \tag{18}$$

The coefficients are listed as follows:

$$g_1 = \frac{(4-5\kappa-2\kappa^2+2\kappa\lambda-11\lambda+4\lambda^2)V''}{4(-1+\kappa+\lambda)^2}, \tag{19}$$

$$g_2 = -\frac{1}{6}V''', \tag{20}$$

$$g_3 = \frac{V'}{2}, \tag{21}$$

$$g_4 = \frac{(-6+25\lambda-24\lambda^2+6\lambda^3+10\kappa-18\kappa\lambda+6\kappa\lambda^2)V'}{8(-1+\kappa+\lambda)^3}, \tag{22}$$

$$g_5 = \frac{(\lambda-1)V'''}{12(-1+\kappa+\lambda)}. \tag{23}$$

The variables in Eq. (18) are changed as follows:

$$T' = g_1 T, \quad R = \sqrt{\frac{g_1}{g_2}}R'. \tag{24}$$

Hence, the mKdV equation can be described as

$$\partial_{T'}R' - \partial_X^3 R' + \partial_X R'^3 + \varepsilon M[R'] = 0, \tag{25}$$

where

$$M[R'] = \frac{1}{g_1}\left[g_3\partial_X^2 R' + g_4\partial_X^4 R' + \frac{g_1 g_5}{g_2}\partial_X^2 R'^3\right]. \tag{26}$$

And then the kink–antikink soliton solution is inferred when we ignore the $O(\varepsilon)$ term as follows:

$$R_0'(X,T') = \sqrt{c}\tanh\left[\sqrt{\frac{c}{2}}(X-cT')\right]. \tag{27}$$

To determine the propagation speed c, $R_0'(XT')$ should meets the following condition:

$$(R_0', M[R']) \equiv \int_{-\infty}^{+\infty} \mathrm{d}X R_0' M[R_0'] = 0. \tag{28}$$

Then, we obtain

$$c = \frac{5g_2 g_3}{2g_2 g_4 - 3g_1 g_5}. \tag{29}$$

Thus, the kink–antikink soliton solution is deduced as given below:

$$\begin{aligned}\Delta x_n(t) \;=\; & h_c + \sqrt{\frac{g_1 c}{g_2}\left(\frac{a_c}{a}-1\right)}\tanh\sqrt{\frac{c}{2}\left(\frac{a_c}{a}-1\right)}\\&\times\left[n+\left(1-cg_1\left(\frac{a_c}{a}-1\right)t\right)\right].\end{aligned} \tag{30}$$

Accordingly, its headway fluctuation amplitude is

$$A = \sqrt{\frac{g_1 c}{g_2}\left(\frac{a_c}{a}-1\right)}. \tag{31}$$

Correspondingly, the coexistence curve can be expressed as

$$\Delta x = h_c \pm A. \tag{32}$$

In view of Eq. (32), we can draw the coexisting line (see the dotted line as shown in Fig. 1). Thereout, we can obtain the conclusion similar to that from the linear analysis, namely, the stability of traffic system can be improved more effectively by taking the CITD effect into consideration.

5. Simulation results

In this section, we will conduct numerical simulation to test the CITD effect on the stability of traffic flow. The purpose of the simulation is to examine the ability of uniform traffic flow to resist small disturbances. We rewrite Eq. (3) into difference form for numerical simulation as follows:

$$\begin{aligned}&\Delta x_n(t+2\tau)\\&= \Delta x_n(t+\tau) + \tau\{V[\Delta x_{n+1}(t) + \kappa(\Delta x_{n+1}(t) - \Delta x_{n+1}(t-\tau))]\\&\quad - V[\Delta x_n(t) + \kappa(\Delta x_n(t) - \Delta x_n(t-\tau))]\}\\&\quad + \lambda\left[\Delta x_n(t+\tau) - 2\Delta x_n(t) + \Delta x_n(t-\tau)\right].\end{aligned} \tag{33}$$

The periodic boundary condition is adopted and the following parameters are selected:

$$N = 100, \quad h_c = 4, \quad v_{\max} = 2, \quad a = 2.67. \tag{34}$$

The initial deviation is set as follows:

$$\begin{cases}\Delta x_n(0) = \Delta x_n(1) = \Delta x_n, & n \neq 0.5N,\ n \neq 0.5N+1,\\ \Delta x_n(0) = \Delta x_n(1) = \Delta x_n - 0.5, & n = 0.5N,\\ \Delta x_n(0) = \Delta x_n(1) = \Delta x_n + 0.5, & n = 0.5N+1.\end{cases} \tag{35}$$

5.1. Headway distribution

The headway distribution can well reflect the stability of the traffic system. If the traffic is stable, then the headways of vehicles are similar to each other. And if there was a traffic jam on the road, then the vehicles would remain a stop-and-go state. So the waves of headway will be jumbled. Hence, we can judge the stability of the traffic system from the volatility of the headway distribution curve. Figure 2 shows the headway distribution diagram of 100 cars at $t = 20300$ time steps. Among them, figures 2(a) and 2(b) show the results of increasing κ and λ, respectively. It can be seen that when $\kappa = 0$ and $\lambda = 0$ (*i.e.* the OV model), the fluctuation amplitude of the headway distribution curve is the maximum. In addition, as κ and λ rise, the volatility of the headway distribution curves also weakens. Especially, the amplitude of headway fluctuation tends to 0 when $\lambda = 0.15$ and $\kappa = 0.05$ and the traffic flow reaches steady state. In short, the CITD effect can stabilize the traffic flow.

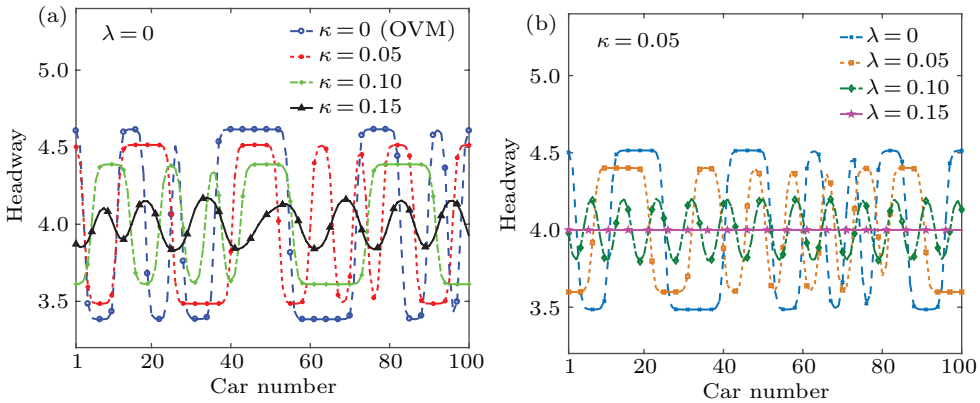


Fig. 2. Headway distribution at the 20300th time step for (a) $\lambda = 0$ and various values of κ, and (b) $\kappa = 0.05$ and various values of λ.

5.2. Hysteresis phenomenon

Figure 3 describes the hysteresis loop composed of headway and headway difference between adjacent time steps (55th car). The abscissa is the headway $\Delta x_{55}(t)$. The vertical coordinate is the headway variation of the 55th car between adjacent time steps. Then, the strength of traffic stability can be judged according to the size of the hysteresis loop. The smaller the area of the hysteretic loop, the better the stability is. Figures 3(a) and 3(b) display the results of augmenting κ and λ, respectively. We can observe that when $\kappa = 0$ and $\lambda = 0$ (*i.e.* the OV model), the area of the hysteretic loop is the largest. This means that the OV model has the severest hysteresis. With the increase of κ and λ, the area of the hysteresis loop is constantly shrinking. In particular, the hysteresis loop contracts to a point when $\lambda = 0.15$ and $\kappa = 0.05$ and all vehicles' headways keep at 4 (m). It shows that the traffic flow is in a steady state at this time. In view of Fig. 3, the stability of the traffic flow is improved by sharing the CITD effect covering both headway and velocity.

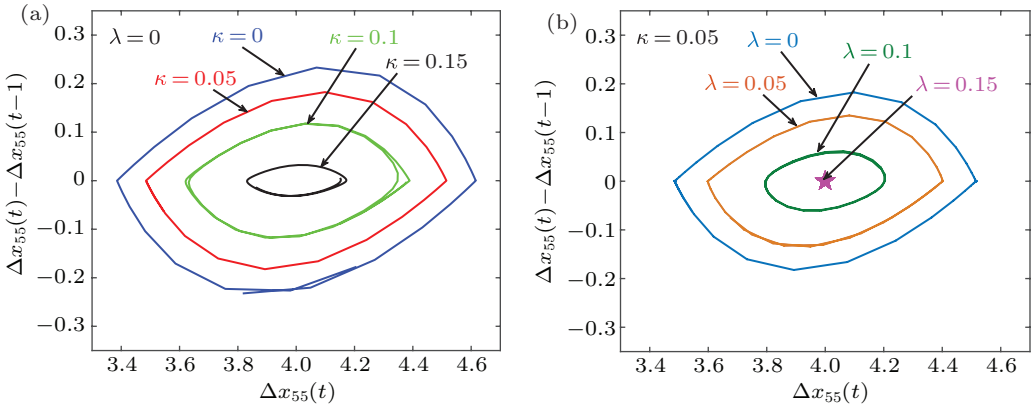


Fig. 3. Hysteresis phenomena (55th car's headway, the headway between adjacent times) for (a) $\lambda = 0$ and various values of κ, and (b) $\kappa = 0.05$ and various values of λ.

5.3. Additional energy consumption

The instantaneous energy consumption is described as[46]

$$\Delta E_n(t) = \frac{1}{2} m_n \left[v_n^2(t+1) - v_n^2(t) \right]. \tag{36}$$

However, the additional energy consumption has not been investigated in the transportation system. In real traffic, the vehicle speed changes little with time for the steady-state traffic flow. The vehicle only needs to maintain a certain stable velocity without frequent braking and acceleration. At this time, the vehicle's kinetic energy remains stable, and the additional energy consumption is wee. On the other hand, the speed of the vehicle can change greatly with time when traffic jam occurs on the road. Cars need to accelerate frequently in the stop-and-go driving process, which greatly aggrandizes the additional energy consumption. Furthermore, we consider that in reality the substantial increase of vehicle's energy consumption does not occur during braking, but usually happens during acceleration.[47] Based on this, in order to better reflect and record the additional energy consumption of a certain car in the acceleration process, we propose

$$\Delta E_n = \sum\nolimits_t \delta_t \frac{1}{2} m_n \left[v_n^2(t+1) - v_n^2(t) \right], \tag{37}$$

where δ_t is a variable factor, when $v_n(t+1) > v_n(t)$, $\delta_t = 1$, otherwise $\delta_t = 0$. By adding δ_t, the additional energy consumption during acceleration can be recorded, while the braking process can be ignored. At the same time, by accumulating time, it can well reflect the total amount of extra energy consumed by a certain car in a period of time. In addition,

on the actual road, different types of vehicles have different amounts of extra energy consumed. It is so complicated to study the amounts of energy consumed by different types of cars. Hence, for better calculation and discussion, in this work all treated vehicles are of the same type and their mass magnitude is set as unit mass 1. Therefore, equation (37) can be rewritten as follows:

$$\Delta E_n = \sum_t \delta_t \frac{1}{2}\left[v_n^2(t+1) - v_n^2(t)\right]. \tag{38}$$

Moreover, in order to better obtain the additional energy consumption of the entire transportation system, we sum up the additional energy consumption of all vehicles (*i.e.* N vehicles) as indicated below:

$$\Delta E = \sum_{n=1}^{N} \Delta E_n. \tag{39}$$

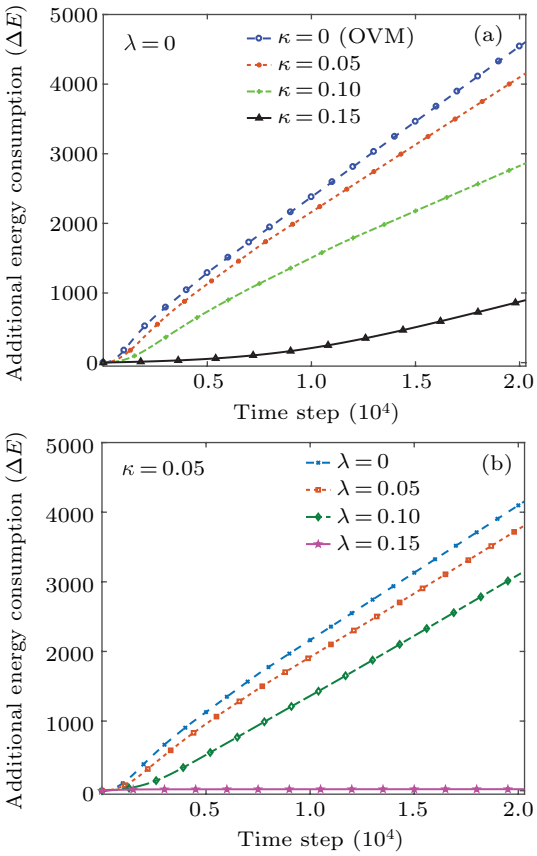


Fig. 4. Additional energy consumption (ΔE) of all vehicles at 20300 time steps for (a) $\lambda = 0$ and various values of κ, and (b) $\kappa = 0.05$ and various values of λ.

Figure 4 shows the curves of additional energy consumption of all vehicles from the beginning to 20300 time steps when κ and λ increase, respectively. The curves of additional energy consumption fall down with κ increasing when $\lambda = 0$ in Fig. 4(a), which proves that the headway delayed effect can reduce the additional energy consumption. And on the basis of Fig. 4(b), the curves of additional energy consumption also show a descending trend as λ aggrandizes when κ is fixed at 0.05. This means that the velocity delayed effect can also cut down the additional energy consumption. Especially when $\kappa = 0.05$ and $\lambda = 0.15$, the additional energy consumption of the entire transportation system tends to 0, which indicates that the traffic flow is already in a steady state in this case. From this experiment it follows that additional energy consumption of overall traffic system is reduced by sharing the CITD effect of headway and velocity under the V2X environment. By means of such traffic optimization, we realize the energy consumption control.

6. Conclusions

In this paper, we present an extended car-following model with the CITD effect covering headway and velocity under the V2X environment. The linear analysis and nonlinear analysis have been executed to explore the stability conditions and the mKdV equation relating to the CITD effect. The numerical simulation experiment further verifies that the CITD effect can alleviate the traffic congestion and improve the stability of traffic flow system. The main conclusions are as follows.

(i) Both the headway delayed effect and the velocity delayed effect can alleviate traffic congestion. When the synergistic function of these two effects is taken into account, the efficiency of the traffic system to reach the steady state can be greatly improved.

(ii) We propose a new method of analyzing the additional energy consumption, which can better illustrate the additional energy consumption of the vehicle during acceleration. It can be found that the additional energy consumption can be effectively controlled macroscopically by considering the CITD effect.

In summary, the synergy of two factors including headway and velocity should be considered at the same time in the car-following model. The car-following model based on the CITD effect can improve the stability of the traffic flow system and reduce additional energy consumption under the V2X environment.

Acknowledgements

Project supported by the National Natural Science Foundation of China (Grant Nos. 61963008, 61673168, 11762004, and 12047567), the Guangxi Natural Science Foundation, China (Grant Nos. 2022GXNSFDA035080 and 2018GXNSFAA281274), the Guangxi Innovation-Driven Development Special Fund Project, China (Grant No. GUIKEAA19254034-3), and the Zhenjiang Science and Technology Project, China (Grant No. GY2020019).

References

[1] Chandler R E, Herman R and Montroll E W 1958 *Oper. Res.* **6** 165
[2] Gazis D C, Herman R and Rothery R W 1961 *Oper. Res.* **9** 545

[3] Bando M, Hasebe K, Nakayama A, Shibata A and Sugoyama Y 1995 *Phys. Rev. E* **51** 1035
[4] Tang T Q, Yi Z Y, Zhang J and Zheng N 2017 *IET. Intell. Transp. Syst.* **11** 596
[5] Zheng Y Z, Zheng P J and Ge H X 2014 *Chin. Phys. B* **23** 020503
[6] Tian J F, Jia B, Li X G and Gao Z Y 2010 *Chin. Phys. B* **19** 010511
[7] Zhang G, Zhao M, Sun D H, Liu W N and Li H M 2016 *Physica A* **442** 532
[8] Zhu W X and Zhang L D 2018 *Physica A* **492** 2154
[9] Ma G Y, Ma M H, Liang S D, Wang Y S and Zhang Y Z 2020 *Commun. Nonlinear Sci. Numer. Simulat.* **85** 105221
[10] Zhao H T, Zhao X, Lu J C and Xin L Y 2020 *J. Comput. Sci-neth.* **47** 101221
[11] Jetto K, Tahiri Z, Benyoussef A and Kenz A E 2020 *Acc. Anal. Prev.* **142** 105507
[12] Kong D W, Sun L S, Li J and Xu Y 2021 *Physica A* **562** 125329
[13] Zeng J W, Qian Y S, Mi P F, Zhang C Y, Yin F, Zhu L P and Xu D J 2021 *Physica A* **562** 125387
[14] Zhao H T, Lin L, Xu C P, Li Z X and Zhao X 2020 *Physica A* **553** 124213
[15] Yang L, Zheng J L, Cheng Y and Ran B 2019 *Physica A* **535** 122277
[16] Nagatani T 1998 *Physica A* **261** 599
[17] Nagatani T 1999 *Physica A* **264** 581
[18] Nagatani T 1999 *Physica A* **265** 297
[19] Wang T, Gao Z Y and Zhao X M 2012 *Chin. Phys. B* **21** 020512
[20] Zhang Y C, Zhao M, Sun D H, Wang S H, Shuai H and Chen D 2021 *Commun. Nonlinear Sci. Numer. Simulat.* **94** 105541
[21] Qin S D, Ge H X and Cheng R J 2018 *Chin. Phys. B* **27** 050503
[22] Li L X, Cheng R J and Ge H X 2021 *Physica A* **561** 125295
[23] Helbing D and Tilch B 1998 *Phys. Rev. E* **58** 133
[24] Jiang R, Wu Q S and Zhu Z J 2001 *Phys. Rev. E* **64** 017101
[25] Backfrieder C, Ostermayer G and Mecklenbrauker C F 2016 *IEEE Trans. Intell. Transp. Syst.* **18** 349
[26] Zhang K L, Yang A S, Su H, De La Fortelle A and Wu X 2016 *IEEE* 19*th Int. Conf. Intel. Trans. Syst.* (ITSC), p. 1192
[27] Ma C X, Hao W, Wang A and Zhao H X 2018 *IEEE Access* **6** 52471
[28] Peng G H, Tang R, Kuang H, Tan H L and Chen T 2021 *Chin. Phys. B* **30** 108901
[29] Ge H X 2011 *Chin. Phys. B* **20** 090502
[30] Jin Y F and Hu H Y 2013 *Commun. Nonlinear Sci. Numer. Simulat.* **18** 1027
[31] Redhu P and Gupta A K 2015 *Commun. Nonlinear Sci. Numer. Simulat* **27** 263
[32] Jin Y F and Meng Xu 2016 *Physica A* **459** 107
[33] Wang Y N, Cheng R J and Ge H X 2017 *Physica A* **479** 478
[34] Peng G H, Yang S H and Zhao H Z 2018 *Physica A* **509** 855
[35] Qin S D, Ge H X and Cheng R J 2018 *Phys. Lett. A* **382** 482
[36] Kaur R and Sharma S 2018 *Physica A* **510** 446
[37] Zhang Y C, Xue Yu, Zhang Peng, Fan D L and He H D 2019 *Physica A* **514** 133
[38] Chang Y Y, He Z T and Cheng R J 2019 *Physica A* **514** 522
[39] Zhang G, Yin L, Pan D B, Zhang Y, Cui B Y and Jiang S 2019 *Physica A* **541** 123704
[40] Jin Y F and Meng J W 2020 *Commun. Nonlinear Sci. Numer. Simulat.* **90** 105333
[41] Li S H, Cheng R J and Ge H X 2020 *Physica A* **558** 125015
[42] Guan X Y, Cheng R J and Ge H X 2021 *Physica A* **574** 125972
[43] Li Z P, Li W Z and Xu S Z 2015 *Nonlinear Dyn.* **80** 529
[44] Nagatani T 1998 *Phys. Rev. E* **58** 4271
[45] Nagatani T 2000 *Phys. Rev. E* **61** 3564
[46] Peng G H, Jia T T, Kuang H and Tan H L 2022 *Physica A* **585** 126443
[47] Oguchi T, Katakura M and Taniguchi M 2002 *J. Jpn. Soc. Civ. Eng.* **695** 125